Volume 14
Number 12
28 March 2023
Pages 3079–3388

Chemical Science

rsc.li/chemical-science

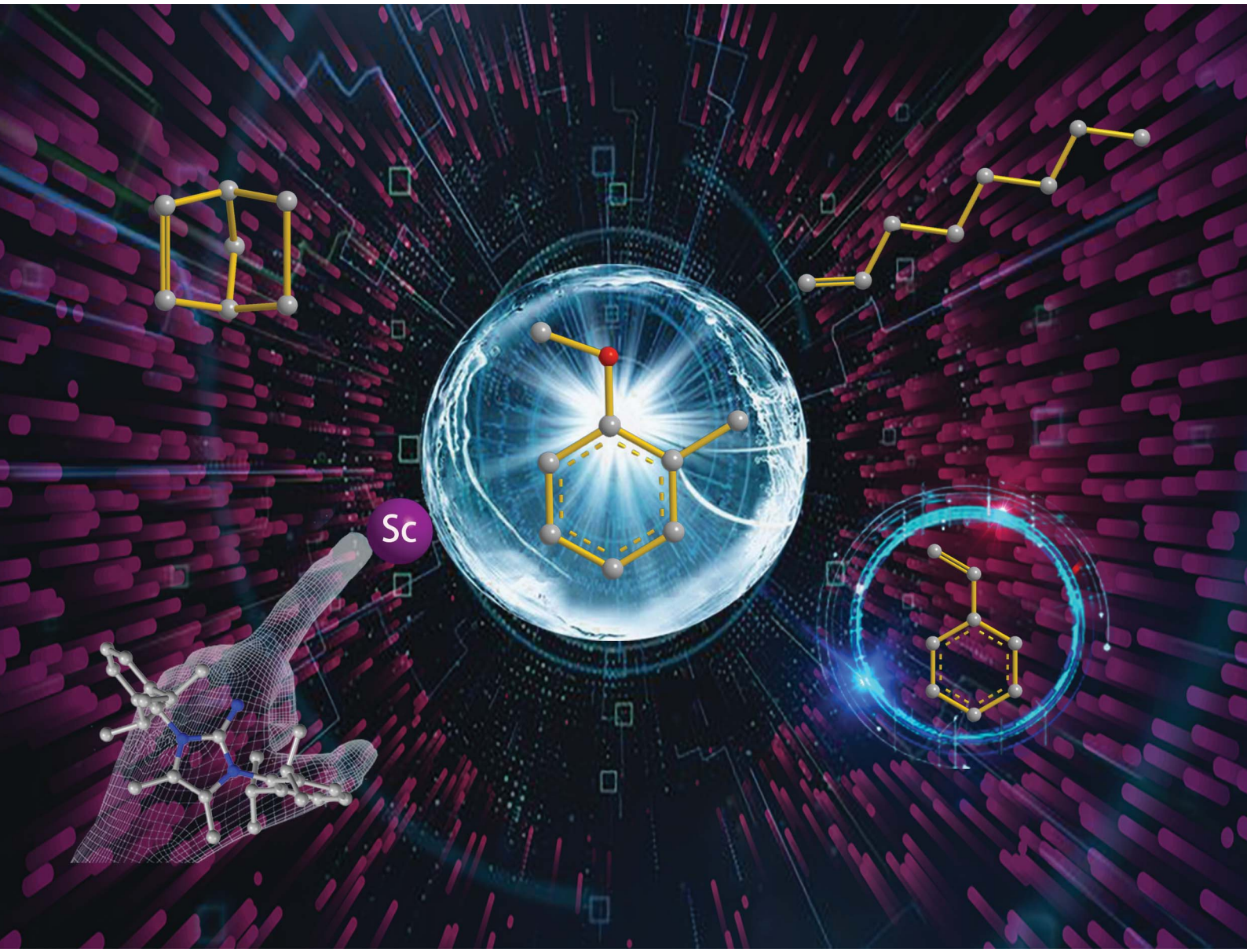

ISSN 2041-6539

ROYAL SOCIETY OF CHEMISTRY

EDGE ARTICLE

Shunxi Dong *et al.*

Regioselective C–H alkylation of anisoles with olefins by cationic imidazolin-2-iminato scandium(III) alkyl complexes

Chemical Science

ROYAL SOCIETY OF CHEMISTRY

EDGE ARTICLE

View Article Online
View Journal | View Issue

Cite this: *Chem. Sci.*, 2023, **14**, 3132

All publication charges for this article have been paid for by the Royal Society of Chemistry

Received 7th December 2022
Accepted 20th January 2023

DOI: 10.1039/d2sc06725k

rsc.li/chemical-science

Regioselective C–H alkylation of anisoles with olefins by cationic imidazolin-2-iminato scandium(III) alkyl complexes†

Shiyu Wang, Chenhao Zhu, Lichao Ning, Dawei Li, Xiaoming Feng and Shunxi Dong *

A new type of rare-earth alkyl complexes supported by monoanionic imidazolin-2-iminato ligands were synthesised and structurally characterised by X-ray diffraction and NMR analyses. The utility of these imidazolin-2-iminato rare-earth alkyl complexes in organic synthesis was demonstrated by their performance in highly regioselective C–H alkylation of anisoles with olefins. With as low as 0.5 mol% catalyst loading, various anisole derivatives without *ortho*-substitution or 2-methyl substituted anisoles reacted with several alkenes under mild conditions, producing the corresponding *ortho*-Csp^2-H and benzylic Csp^3-H alkylation products in high yield (56 examples, 16–99% yields). Control experiments revealed that rare-earth ions, ancillary imidazolin-2-iminato ligands, and basic ligands were crucial for the above transformations. Based on deuterium-labelling experiments, reaction kinetic studies, and theoretical calculations, a possible catalytic cycle was provided to elucidate the reaction mechanism.

Introduction

Anisole and its derivatives are frequently occurring structural units in many pharmaceuticals, natural products, and functional materials.[1] The development of succinct and efficient approaches for the production of anisoles and their derivatives has therefore attracted significant interest in the past few decades.[2–5] In particular, the C–H alkylation of anisoles with alkenes represents one of the most atom-efficient and environmentally benign synthetic routes.[2–4] Although the well-known Friedel–Crafts type reactions of anisoles with alkenes *via* carbocation intermediates have been extensively investigated with Lewis and Brønsted acids as the catalysts, the control of regioselectivity has been problematic; a mixture of *ortho*- and *para*-regioisomers are always concomitantly generated in the reaction process (Scheme 1a).[2] The metal–organic complex-mediated C–H alkylation of anisoles with alkenes *via* C–H activation is an alternative pathway to obtain alkylated anisoles.[3,4] However, owing to the weak interaction between late-transition metals and the ether moiety, the use of transition metal-based catalysts in such transformations is fruitless.[6] In contrast, rare-earth organic complexes benefit from their unique chemical properties and have been successfully disclosed to be efficient promoters by Hou and others.[3] Taking advantage of the strong oxophilicity of rare-earth metal ions and their high activity towards olefin migration insertion, Hou and co-workers first accomplished intermolecular and intramolecular C–H bond addition of anisoles to various alkenes with cationic half-sandwich yttrium(III) or scandium(III) alkyl complexes as the catalysts (**cat-1** and **cat-2**; Scheme 1b, left).[3a,c] In 2019, the group of Chen extended alkene substrates to 1,5-dienes and 1,6-dienes under the influence of cationic 2-picoline-tether-half-sandwich scandium(III) alkyl catalyst (**cat-3**). The cyclisation/hydroarylation reaction of aromatic ethers took place successfully, delivering several anisole derivatives in good yield with high regio- and diastereoselectivity (Scheme 1b, right).[3b] Overall, despite such impressive advances in this field, there is still ample room for improvement in terms of new catalysts and product distribution.

Rare-earth organic complexes have been emerging as competent catalysts for several important organic transformations,[7] including C–H functionalisation[8] and polymerisation reactions.[9] The development of this area, in particular C–H functionalisation, heavily relies on the use of cyclopentadienyl (Cp) and its analogues as ancillary ligands. The quest for alternatives of Cp and related aromatic ligands is of great interest and significance, but has met with limited success to date.[10] Among them, *N*-heterocyclic iminato (NHI) ligands, for example, monoanionic imidazolin-2-iminato groups, have been successfully investigated as Cp-analogous ligands by the groups of Tamm, Inoue, Eisen, and others.[11] Structurally, imidazolin-2-iminato groups are isolobally related to the Cp moiety. As shown in Scheme 2a, the two mesomeric structures

Key Laboratory of Green Chemistry & Technology, Ministry of Education, College of Chemistry, Sichuan University, Chengdu 610064, China. E-mail: dongs@scu.edu.cn

† Electronic supplementary information (ESI) available: ^1H, $^{13}C\{^1H\}$ and $^{19}F\{^1H\}$ NMR. X-ray crystallographic data. CCDC [2219241–2219245]. For ESI and crystallographic data in CIF or other electronic format see DOI: https://doi.org/10.1039/d2sc06725k

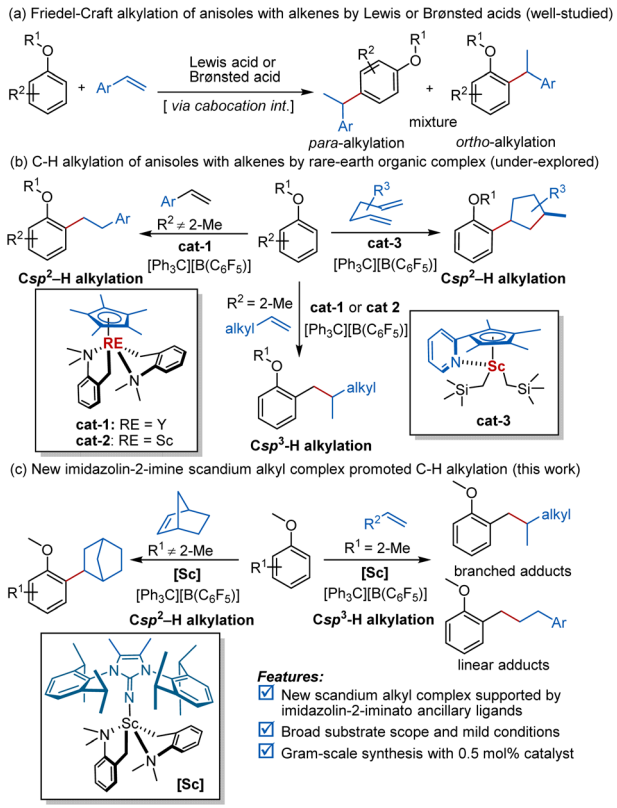

Scheme 1 Catalytic synthesis of anisoles derivatives through C–H alkylation of anisoles with alkenes.

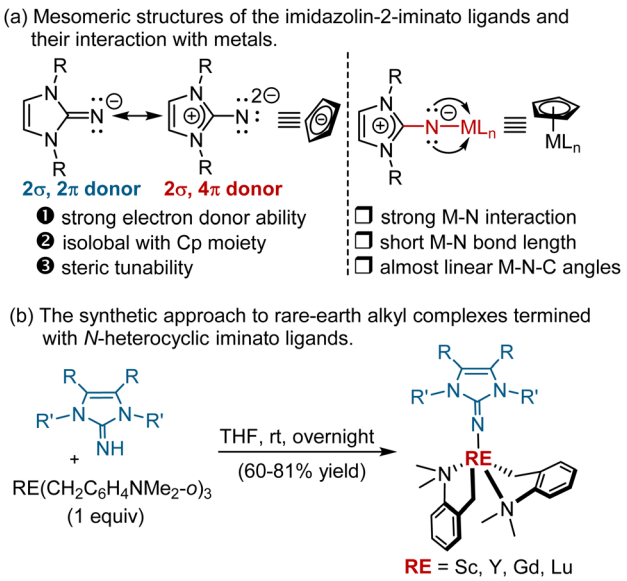

Scheme 2 (a) The structural features of *N*-heterocyclic iminato ligands; and (b) synthetic method for their rare-earth alkyl complexes.

of the imidazolin-2-iminato groups indicated that they can serve as strong 2σ,4π-electron N-donor ligands (Scheme 2a).[12] Thanks to their strong electron donation and steric tunability, the related imidazolin-2-iminato rare-earth alkyl complexes exhibit high activity toward several reactions, including hydroamination,[13] hydrosilylation,[13] nucleophilic addition,[14] and polymerisation.[15] Nevertheless, it remains unclear whether imidazolin-2-iminato rare-earth alkyl complexes could be used in C–H activation. Motivated by the distinct selectivity and functional group tolerance frequently shown in rare-earth mediated C–H functionalisation[8] and elegant work[11] from Tamm's group, we envisaged that the judicious choice of rare-earth ions and basic ligands, as well as modification of imidazolin-2-iminato supporting ligands, may have the potential to achieve C–H alkylation with olefins. Herein, we wish to disclose our preliminary results along this line. An array of imidazolin-2-iminato rare-earth alkyl complexes were synthesised and structurally characterised by X-ray diffraction and NMR analyses. The cationic imidazolin-2-iminato scandium(III) alkyl complex was eventually identified as an efficient catalyst for highly regioselective C–H alkylation of anisole with *ortho*-Csp^2-H and 2-methylanisole with Csp^3-H (0.5–10 mol% catalyst loading, 56 examples, 16–99% yield). Notably, in comparison with cationic half-sandwich rare earth alkyl catalyst, a different catalytic performance was observed with these newly designed rare-earth metal complexes obtained from the reaction of 2-methylanisoles with styrenes.[3a] In addition, a possible catalytic cycle has been provided to understand the reaction mechanism based on deuterium-labelling experiments, reaction kinetic studies, and DFT calculations.

Results and discussion

To validate the feasibility of the hypothesis, we first prepared a set of imidazolin-2-iminato rare-earth alkyl complexes by acid–base reaction of homoleptic tris(aminobenzyl) rare-earth complex $RE(CH_2C_6H_4NMe_2\text{-}o)_3$ and 1 equivalent of imidazolin-2-imine[16] in THF at room temperature for 12 h (Scheme 2b). The molecular structure of **Sc-1**, **Sc-2**, **Y-1**, and **Gd-1** were established by single crystal X-ray diffraction analysis. As shown in single crystal structures, extremely short metal-nitrogen bonds [Sc–N: 1.956(4) Å, 1.971(3) Å, Y–N: 2.104(2) Å, Gd–N: 2.147(2) Å] and almost linear M-N-C angles (178.1–178.9°) were observed.[17] To better understand the nature of the Sc–N bond, the bond order, localised molecular orbitals, and canonical molecular orbitals analysis were performed with Multiwfn software (see ESI† for more details). As depicted in Fig. 1a, the calculated Wiberg bond order of Sc–N is 1.36,[18] indicating a strong interaction between the N atom of NHI and the scandium(III) ion. The decomposing Mayer bond order (MBO) analysis shows that one σ and two π orbitals contribute to the Sc–N bond. The molecule orbital analysis of **Sc-1** also disclosed that except for the existence of one σ-bond, two p orbitals of the N atom in NHI form two π bonds with two d orbitals of the Sc ion, respectively, providing further evidence for their capability of acting as 2σ,4π-electron donors (Fig. 1b–d). The calculated ADCH charges suggested the charge donation from the NHI to the scandium(III) centre is −0.91 (for more details, see ESI†).

To investigate the catalytic activity of the newly designed imidazolin-2-iminato rare earth alkyl complexes, we conducted anisole Csp^2-H alkylation and 2-methylanisole benzyl Csp^3-H

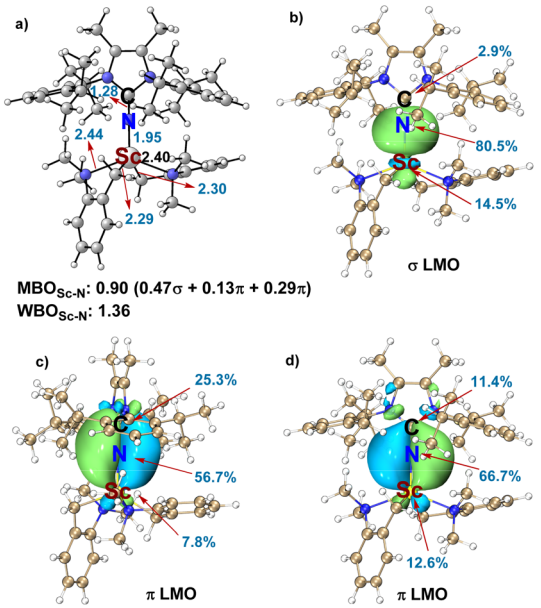

Fig. 1 The Mayer bond order (MBO), Wiberg bond order (WBO), and the localised molecular orbitals of σ and π bond between the Sc and N atoms in the catalyst **Sc-1** (isovalue = 0.02).

alkylation with alkenes. Initially, the reaction of methyl phenyl ether (**1a**) with norbornene (**2a**) was selected as the model reaction for optimisation. As summarised in Table 1, the rare-earth ions displayed a significant effect on the activity of catalysts. With 2.5 mol% imidazolin-2-iminato scandium bis(aminobenzyl) complex **Sc-1** as the catalyst, the reaction of **1a** and **2a** underwent well in toluene at 50 °C for 24 h, affording the corresponding *ortho*-alkylation product **3aa** in 99% yield (Table 1, entry 1). In stark contrast, no reaction was detected for its analogues, such as yttrium (**Y-1**), gadolinium (**Gd-1**), or lutecium (**Lu-1**) (entry 2). The effect of ligand structure on catalytic activity was examined. Changing 4,5-dimethyl groups on the skeleton of the imidazolin-2-imine ring to 4,5-dichloride presented comparable activity (entry 3, 99% yield). Decreasing the steric hindrance of the aromatic group on nitrogen atoms from 2,6-^{i}Pr$_2$ to 2,4,6-Me$_3$ or replacing 2,6-^{i}Pr$_2$C$_6$H$_3$ with 1-adamantyl substitution led to no product. No reaction was observed with 1,3-bis(2,4,6-trifluorophenyl)imidazolidin-2-imine-derived **Sc-5** (entry 4). **Sc-6** with bis(noesilyl) [CH$_2$Si(CH$_3$)$_3$] basic ligand also performed well with 99% yield (entry 5).[19] Switching **Sc-1** to tris(aminobenzyl) scandium(III) **Sc-7** resulted in an obvious decrease in yield (entry 6). Performing the reaction without [Ph$_3$C][B(C$_6$F$_5$)$_4$] led to a full loss of activity (entry 7). Running the reaction without **Sc-1** resulted in an obvious decrease in yield (entry 8). These results suggested that the cationic imidazolin-2-iminato scandium(III) alkyl complex was probably the real catalytic active species, and the presence of imidazolin-2-iminato ligand was crucial for the high activity observed. Next, other reaction parameters were studied (for more details, see ESI†). It was found that the reaction took place well in *n*-hexane, and 86% yield was obtained (entry 9). The coordinative solvents, for example, THF, inhibited the reaction (entry 10). When the reaction was carried out at a higher temperature (70 °C), an excellent yield was obtained (entry 11). A further decrease in temperature to 40 °C led to reduced yield (entry 12, 88% yield). Performing the reaction with 2 mol% of catalyst provided a slightly lower yield (91% *vs.* 99%). Further decrease in the catalyst loading to 1 mol% led to severe erosion in yield (entries 14, 47% yield).

With the optimum reaction conditions in hand, we assessed the reactions of norbornene with various anisoles in the presence of **Sc-1** (Scheme 3). Anisoles with different substituents at the *para*- and *meta*-position of the phenyl ring were all compatible in the current system, yielding the related *ortho*-alkylation products **3aa–3ia** in 86–99% yields. Halide atoms (F, Cl, Br, I) at the *para*-position of the phenyl ring were retained

Table 1 Screening of the reaction conditions of anisole **1a** with norbornene **2a** [a]

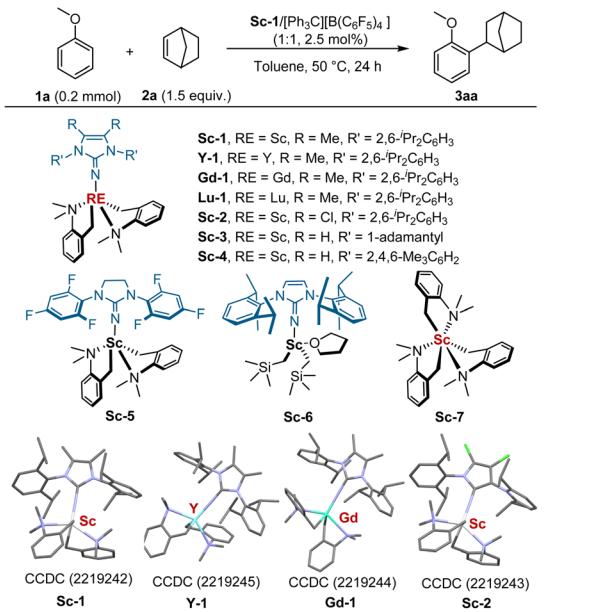

Entry	Deviations	Yield (%)[b]
1	None	99 (99)
2	10 mol% **Y-1**, **Gd-1** or **Lu-1**	NR
3	10 mol% **Sc-2**	99
4	10 mol% **Sc-3**, **Sc-4** or **Sc-5**	NR
5	10 mol% **Sc-6**	99
6	10 mol% **Sc-7**	37
7	No [Ph$_3$C][B(C$_6$F$_5$)$_4$]	NR
8	No **Sc-1**	30
9	*n*-hexane	86
10	THF	NR
11	70 °C	94 (94)
12	40 °C	88
13	2 mol% **Sc-1**	91 (90)
14	1 mol% **Sc-1**	47 (45)

[a] Standard conditions: **Sc-1**/[Ph$_3$C][B(C$_6$F$_5$)$_4$] (1 : 1, 2.5 mol%), **1a** (0.20 mmol), **2a** (0.30 mmol) in toluene at 50 °C for 24 h. [b] Yield was determined by 1H NMR with C$_2$H$_2$Br$_4$ as an internal standard. Yield in brackets refers to isolated yield.

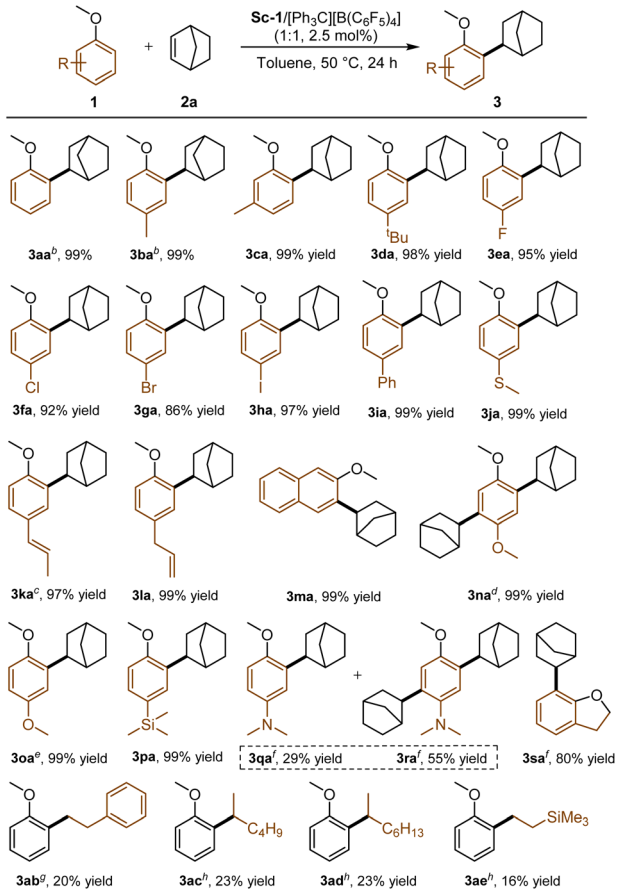

Scheme 3 Substrate scope of anisoles. [a]Unless otherwise noted, all reactions were performed with **Sc-1**/$[Ph_3C][B(C_6F_5)_4]$ (1 : 1, 2.5 mol%), **1** (0.20 mmol), **2a** (0.60 mmol) in toluene (0.5 mL) at 50 °C for 24 h. [b]**2a** (0.30 mmol). [c]5 mol% catalyst. [d]5 mol% catalyst, 36 h. [e]5 mol% catalyst, **1** (0.20 mmol), **2a** (0.20 mmol), 36 h. [f]10 mol% catalyst, **1** (0.20 mmol), **2a** (1.20 mmol), 100 °C. [g]10 mol% catalyst, **1a** (0.30 mmol), **2** (0.20 mmol). [h]10 mol% catalyst, **1a** (0.20 mmol), **2** (2.00 mmol).

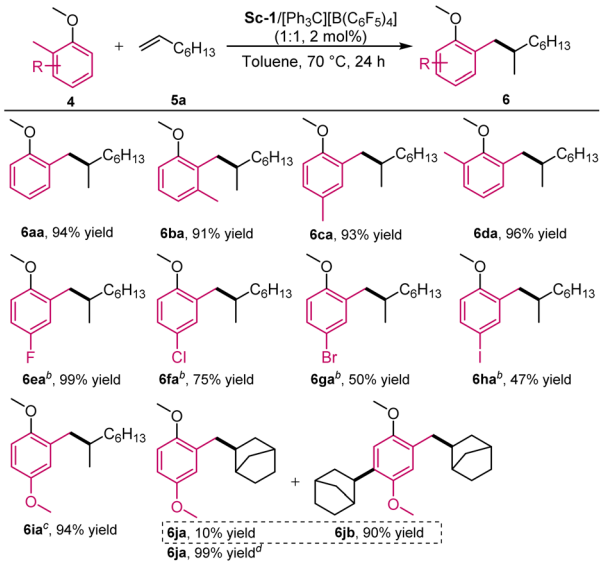

Scheme 4 Substrate scope of 2-methylanisole. [a]Unless otherwise noted, all reactions were performed with **Sc-1**/$[Ph_3C][B(C_6F_5)_4]$ (1 : 1, 2.0 mol%), **4** (0.20 mmol), **5a** (0.60 mmol) in toluene (0.5 mL) at 70 °C for 24 h. The yield of isolated product. [b]10 mol% catalyst. [c]5 mol% of catalyst. [d]Carried out with **4a** (0.30 mmol), norbornene **2a** (0.20 mmol).

after the reaction (**3ea–3ha**), which is different from the late-transition metals catalytic system.[20] The reaction of the substrate with the 4-SMe group exclusively took place at the *ortho*-position of OMe in 99% yield (**3ja**), which was probably due to the strong oxophilicity of rare-earth metals. The anisoles bearing vinyl or allylic substitutions were well-tolerated as well, affording the corresponding adducts **3ka** and **3la** in 97 and 99% yields, respectively. In cases of *meta*-methyl anisole and 2-methoxynaphthalene, which have two different *ortho*-C–H bonds, the alkylation selectively occurred at less sterically congested positions (**3ca** and **3ma**, 99% yields for both). For the reaction of anisole with the 4-OMe group, the increase in catalyst loading (5 mol% and prolonged reaction time 36 h) were necessary to get good results, and the NMR spectra indicated that the dialkylation adduct **3na** was obtained (99% yield). Carrying out the reaction with 1 equivalent of norbornene led to the formation of monoalkylation product **3oa** in 99% yield. The trimethylsilyl group at *para*-position also performed well with 99% yield (**3pa**). When 4-methoxy-*N*,*N*-dimethylaniline was used as the reaction partner, monoalkyation (**3qa**, 29%) and dialkylation adducts (**3ra**, 55%) were obtained. 2,3-Dihydrobenzofuran transformed into the product **3sa** smoothly with 10 mol% catalyst loading (80% yield). Unfortunately, the reactions of methyl phenyl ether with other alkenes, such as styrene, 1-hexene, 1-octene, and vinyl trimethylsilane, were sluggish, and only low yields were obtained (16–23% yields). When other alkyl phenyl ethers, for instance, ethyl phenyl ether, were subjected to standard conditions, no reaction occurred at all (see ESI, Page 11 for more details†).

Encouraged by the above results, we extended the substrates to 2-methyl substituted anisoles. As illustrated in Scheme 4, with 2 mol% of **Sc-1**, 2-methyl substituted anisole (**4a**) reacted with 1-octene effectively at 70 °C for 24 h, and the desired benzylic Csp^3-H alkylation product **6aa** was isolated in 94% yield (for detailed optimisation, see ESI, Pages 12 and 13†). The scope of 2-methylanisoles was then investigated. 2-Methyl-substituted anisoles with an additional methyl substituted at 3-, 4-, or 6-positions of the phenyl ring were amenable to the reaction, yielding branched C–H alkylation products **6ba–6da** in 91–96% yields. The reactions of halide atoms substituted substrates were sluggish, and higher catalyst loading (10 mol%) was used. From fluorine to iodine, the isolated yield decreased gradually (**6ea–6ha**, 99 → 47%). In the case of 4-OMe substituted one, benzylic Csp^3-H alkylation preferred to take place rather than *ortho*-Csp^2-H alkylation (**6ia**, 94% yield), which was different from the previous report by Hou and co-workers.[3a] The use of norbornene instead of 1-octene led to a mixture of benzylic Csp^3-H alkylation adduct **6ja** and dialkylation product **6jb** (*ca.* 1 : 9 ratio). Performing the reaction with 1.5 equivalents of 1,4-dimethoxy-2-methylbenzene provided **6ja** as the sole product in 99% yield.

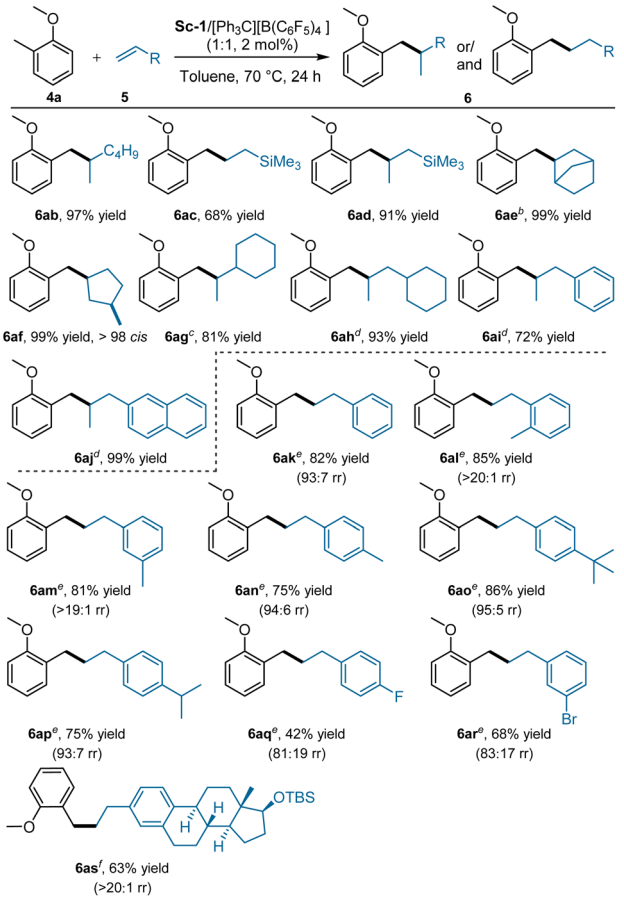

Scheme 5 Substrate scope of alkenes. [a]Unless otherwise noted, all reactions were performed with **Sc-1**/[Ph_3C][$B(C_6F_5)_4$] (1 : 1, 2 mol%), **4a** (0.20 mmol), **5** (0.60 mmol) in toluene (0.5 mL) at 70 °C for 24 h. The yield of isolated product. [b]0.5 mol% catalyst. [c]5 mol% catalyst. [d]10 mol% catalyst. [e]Run with 10 mol% catalyst, **4a** (0.10 mmol), **5** (0.15 mmol). Yield of isolated linear product. [f]Carried out with 10 mol% catalyst, **4a** (0.15 mmol), **5** (0.10 mmol).

Next, diverse alkenes were evaluated with 2-methyl substituted anisole (**4a**). Alkyl-substituted alkenes, such as 1-hexene, allyltrimethylsilane, and norbornene, were all suitable, affording branched benzyl Csp^3-H alkylation products (**6ab**, **6ad**, and **6ae**) in 91–99% yields (Scheme 5). Notably, the use of vinyltrimethylsilane generated the linear product **6ac** in 68% yield due to the ability of silicon to aid the stabilisation of negative charge.[21] In the case of 1,5-hexadiene, continuous 2,1-insertion resulted in hydroalkylation and cyclisation product **6af** in 99% yield with >98 *cis*. Vinyl cyclohexane was subjected to the reaction, branched product **6ag** was produced in 81% yield. The present reaction was applicable for allyl cyclohexane, allylbenzene, and 2-allylnaphthalene as well, giving the corresponding products **6ah–6aj** in 72–99% yields. In Hou's work,[3a] no reaction of 2-methylanisole with styrene occurred in the presence of a half-sandwich rare-earth complex. To our delight, styrene and its derivatives were feasible in the current reaction system, and linear products were generated as the major products with a variable amount of branched adducts.[21] As shown in Scheme 5, the bottom part, *ortho*-, and *meta*-methyl

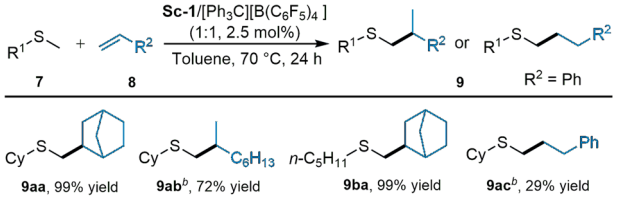

Scheme 6 Substrate scope of sulfides. [a]Unless otherwise noted, all reactions were performed with **Sc-1**/[Ph_3C][$B(C_6F_5)_4$] (1 : 1, 2.5 mol%), **7** (0.20 mmol), **8** (0.60 mmol) in toluene (0.5 mL) at 70 °C for 24 h. The yield of isolated product. [b]10 mol% catalyst, **7a** (1.0 mmol), **8** (0.20 mmol).

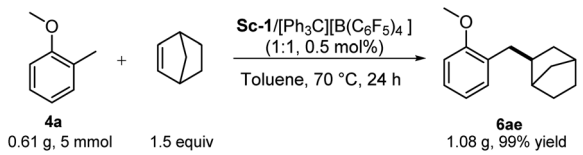

Scheme 7 Gram-scale synthesis of **6ae**.

substituted styrenes provided higher yield than *para*-substituted ones due to the formation of less amount of branched by-products (85 and 81% yield *vs.* 75% yield). Relatively lower yields (**6aq**: 42% yield; **6ar**: 68% yield) were afforded for the reaction of styrenes with fluoro or bromine groups than those of other alkyl groups. Olefins derived from estradiol also transformed into the related product **6as** in moderate yield (63%).

In addition, sulfides were feasible as well in the current reaction system.[22] As shown in Scheme 6, high yields (**9aa:** 99% yield; **9ba:** 99% yield) were obtained for the reaction of cyclohexyl(methyl)sulfane and methyl(pentyl)sulfane with norbornene. Vinyl cyclohexane converted into the related branched product **9ab** with 72% yield. The reaction of styrene afforded the linear product **9ac** in low yield (29%).

To further demonstrate the synthetic utility of this protocol, a gram–scale reaction was conducted. As shown in Scheme 7, the reaction of 5 mmol of **4a** with 1.5 equivalents of **2a** in the presence of 0.5 mol% of **Sc-1** proceeded smoothly, furnishing the corresponding benzyl Csp^3-H alkylation product **6ae** in 99% isolated yield (1.08 g) (Scheme 7).

To gain further insights into the mechanism of Csp^2-H alkylation of anisole and benzyl Csp^3-H alkylation of 2-methylanisole, a series of deuterium-labelling and kinetic studies were carried out. Intramolecular KIE experiment of deuterium-labelled 4-methyl[2-D]anisole (**1b-D**) with norbornene (**2a**) showed a significant kinetic isotope effect (KIE) value of 5.2 (Scheme 8a), indicating that Csp^2-H cleavage of anisole might be involved in the turnover limiting step. In Hou's work, an intramolecular kinetic isotopic effect was not observed (k_H/K_D = 1) in the reaction with styrene.[3a] Two sets of intermolecular KIE experiments of 2-methylanisole and 1-methoxy-2-(methyl-d_3) benzene react with norbornene or 1-octene mixed in 1 : 1 : 3 molar ratio showed a significant kinetic isotope effect (KIE) value of 4.5 and 5.7, respectively (Scheme 8b and 8d). Two sets

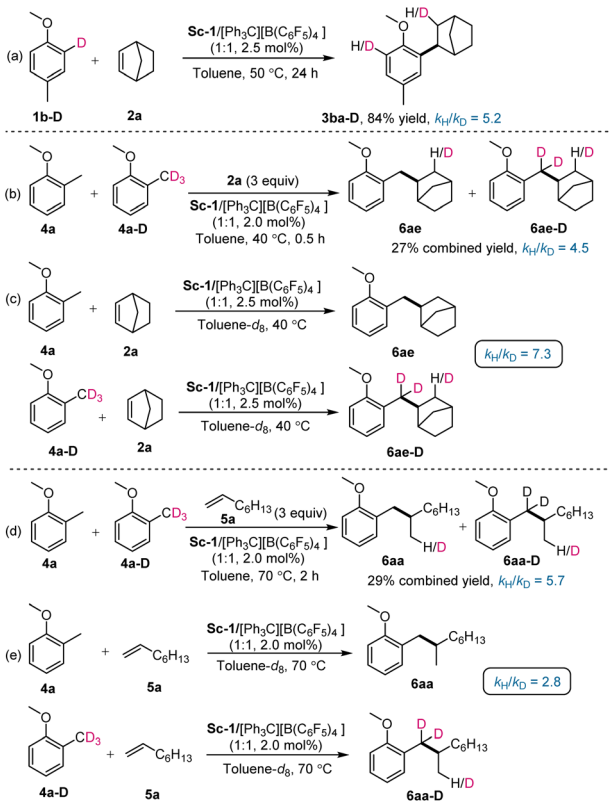

Scheme 8 Deuterium-labelling experiments.

of parallel reactions were conducted and KIE values of 7.3 and 2.8 were observed (Scheme 8c and 8e). The above outcomes suggested that benzyl Csp^3-H cleavage of 2-methylanisole might be involved in the turnover-limiting step as well. In addition, we measured the rate concentration dependences of 2-methylanisole (**4a**), 1-octene (**5a**), and catalyst precursor **Sc-1**. It was found that the reaction showed a first-order rate dependence on the concentration of **4a** and the catalyst. Interestingly, the concentration of **5a** also affected the reaction rate, an approximate first-order rate (0.75) dependence on the **5a** concentration was observed. Overall, the reaction rate was affected by the concentration of 2-methylanisole (**4a**), 1-octene (**5a**), and the catalyst precursor **Sc-1**.

To understand the reaction mechanism, theoretical calculations were performed by using **Sc-1** in the formation **6aa**. The detailed results, including Gibbs free energy profiles and structures, are summarised in Fig. 2. Initially, the catalyst precursor **Sc-1** reacted with $[Ph_3C][B(C_6F_5)_4]$ to generate the corresponding cationic scandium alkyl species, which was confirmed by ^1H NMR analysis.[23] The coordination of the methoxy group of **4a** to scandium(III) provided the cationic scandium species, followed by selective deprotonation at benzylic position afforded the five-membered metallacycle intermediate **INT1** through σ-bond metathesis, which was thought to be the real catalytic active species. According to the energy profile, the pathway involving another 2-methylanisole *via* **TS1** (9.8 kcal mol^{-1}) was more favoured than the other pathway *via* **TS1'** (15.2 kcal mol^{-1}).[24] Then, the simultaneous coordination of **INT1** with another **4a** and 1-octene (**5a**) furnished **INT2**, which subsequently underwent 1,2-insertion of **5a** into the Sc–C bond in **INT2** to give rise to intermediate **INT3** *via* the transition state **TS1**. This process needed to overcome an energy barrier of 9.8 kcal mol^{-1}. In contrast, the 2,1-insertion of 1-octene into the Sc–C bond in INT2 was unfavoured in terms of the energy barrier (12.0 kcal mol^{-1} *vs.* 9.8 kcal mol^{-1}). In comparison, the DFT calculation suggested that the energy barrier of 1,2-insertion of styrene into the Sc–C bond was slightly higher than that of 2,1-insertion (10.9 kcal mol^{-1} *vs.*

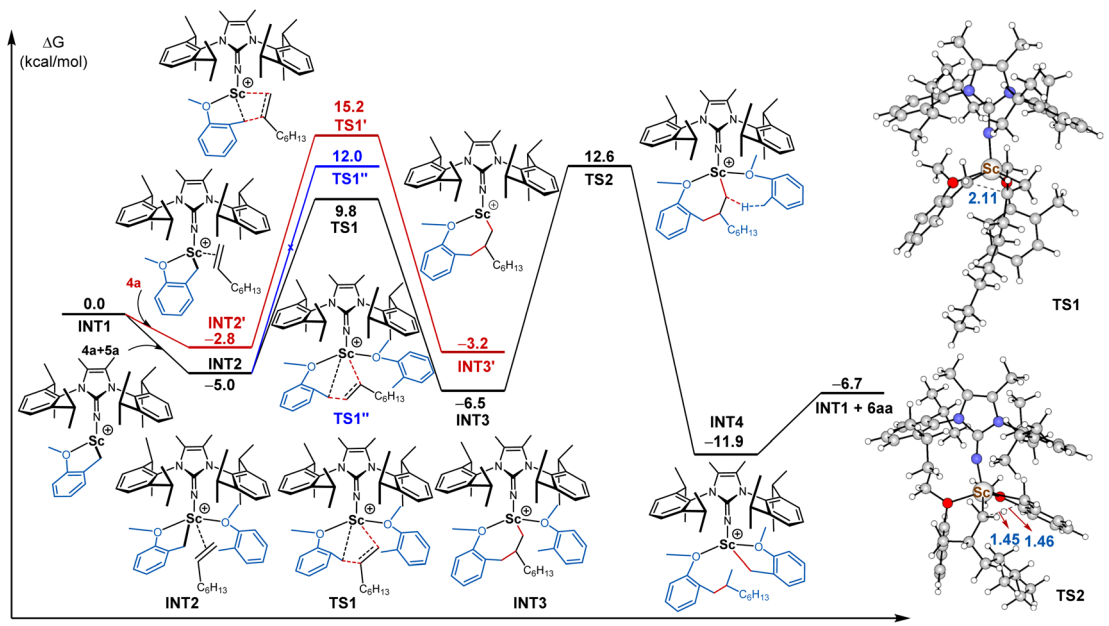

Fig. 2 Energy profile for the regioselective benzylic Csp^3-H alkylation of **4a** with **5a**.

11.6 kcal mol^{-1}, see ESI† for more details). The above results provide a rational explanation for the regioselectivity observed in experimental studies in Schemes 4 and 5. Upon activating the benzylic Csp^3-H bond of another molecule **4a**, intermediate **INT4** was generated with an activation barrier of 12.6 kcal mol^{-1}. Finally, **INT4** liberated the desired product **6aa** and regenerated catalytic species **INT1**. Although the turnover limiting step was identified to be the Csp^3-H activation step, the activation barriers *via* **TS1** and **TS2** were similar. Therefore, the concentration of alkene substrate had an obvious effect on the reaction rate as well, which was in agreement with kinetic results. In addition, the calculated KIE value (k_H/k_D) was 3.7, which was consistent with the KIE experimental result.

Next, the reaction of 1,4-dimethoxy-2-methylbenzene (**4i**) with 1-octene (**5a**) was studied by DFT calculations to further clarify the regioselectivity (see ESI† for more details). The results indicated that the Csp^3-H activation pathway is more favourable than the Csp^2-H activation pathway for the 1,4-dimethoxy-2-methylbenzene kinetically and thermodynamically. Therefore, only the Csp^3-H alkylation product was obtained in the current reaction system.

Conclusions

A new type of imidazolin-2-iminato rare earth alkyl complexes was prepared and successfully employed as competent catalysts for C–H alkylation of anisoles and 2-methylanisoles with various alkenes. A series of anisole derivatives were obtained under mild conditions with high regioselectivity and yield. The experimental results indicated that the activation of the benzylic Csp^3-H bond is preferred to that of *ortho*-Csp^2-H in an aromatic ring. Rare-earth ions, ancillary imidazolin-2-iminato ligands, base ligands, and borate play a significant role in the titled transformations. Based on deuterium-labelling experiments, reaction kinetic studies, and DFT calculations, a catalytic cycle along with possible working modes were provided under the reaction mechanism. The development of chiral imidazolin-2-iminato rare earth alkyl complexes and their further utility in other related C–H alkylation reactions are in progress.[25]

Data availability

The data supporting this article has been uploaded as part of the ESI.†

Author contributions

S. Y. Wang performed experiments and prepared the ESI† and paper. C. H. Zhu repeated some experiments. L. C. Ning carried out the DFT calculations. D. W. Li helped with crystal growth. X. M. Feng and S. X. Dong supervised the project and polished the manuscript and ESI.†

Conflicts of interest

There are no conflicts to declare.

Acknowledgements

We are grateful for the financial support from the National Natural Science Foundation of China (No. 92056107, 22271199, 92256303 and 21890723) and Sichuan University (2020SCUNL204).

Notes and references

1 For selected examples of valuable molecules containing anisole moiety, see: (*a*) S. Shiotani, T. Kometani, K. Mitsuhashi, T. Nozawa, A. Kurobe and O. Futsukaichi, *J. Med. Chem.*, 1976, **19**, 803; (*b*) T. Pacher, C. Seger, D. Engelmeier, S. Vajrodaya, O. Hofer and H. Greger, *J. Nat. Prod.*, 2002, **65**, 820; (*c*) L. Garrido, E. Zubía, M. J. Ortega and J. Salvá, *J. Org. Chem.*, 2003, **68**, 293; (*d*) M. A. Grundl and D. Trauner, *Org. Lett.*, 2006, **8**, 23; (*e*) T. Zhou, Q. Shi, K. F. Bastow and K.-H. Lee, *J. Med. Chem.*, 2010, **53**, 8700; (*f*) R. Gaspari, A. E. Prota, K. Bargsten, A. Cavalli and M. O. Steinmetz, *Chem*, 2017, **2**, 102; (*g*) Z.-S. Liu, G.-G. Qian, Q.-W. Gao, P. Wang, H.-G. Cheng, Q. Wei, Q. Liu and Q.-H. Zhou, *ACS Catal.*, 2018, **8**, 4783; (*h*) G. A. Pakora, J. Mpika and D. Kone, *Environ. Sci. Pollut. Res.*, 2018, **25**, 29901; (*i*) L. Chen, M. P. Pu, S. Y. Li, X. P. Sang, X. H. Liu, Y. D. Wu and X. M. Feng, *J. Am. Chem. Soc.*, 2021, **143**, 19091; (*j*) Y. Li, S. Xin, R. Weng, X. H. Liu and X. M. Feng, *Chem. Sci.*, 2022, **13**, 8871; (*k*) Y. Xu, H. K. Wang, Z. Yang, Y. Q. Zhou, Y. B. Liu and X. M. Feng, *Chem*, 2022, **8**, 2011.

2 For selected examples of hydroalkylation of anisole *via* Friedel-Craft type reactions, see: (*a*) H.-B. Sun, B. Li, R.-M. Hua and Y.-W. Yin, *Eur. J. Org. Chem.*, 2006, **18**, 4231; (*b*) S. Y. Lee, A. V. Gale and C. C. Eichman, *Org. Lett.*, 2016, **18**, 5034; (*c*) R. K. Nandi, F. Ratsch, R. Beaud, R. Guillot, C. Kouklovskya and G. Vincent, *Chem. Commun.*, 2016, **52**, 5328; (*d*) J. N. Bentley and C. B. Caputo, *Organometallics*, 2018, **37**, 3654; (*e*) C. D. T. Nielsen, A. J. P. White, D. Sale, J. Bures and A. C. Spivey, *J. Org. Chem.*, 2019, **84**, 14965.

3 (*a*) J. Oyamada and Z. Hou, *Angew. Chem., Int. Ed.*, 2012, **51**, 12828; (*b*) B. Tang, X.-Y. Hu, C.-L. Liu, T. Jiang, F. Alam and Y.-H. Chen, *ACS Catal.*, 2019, **9**, 599; (*c*) A. Mishra, P. Wu, X.-F. Cong, M. Nishiura, G. Luo and Z. Hou, *ACS Catal.*, 2022, **12**, 12973.

4 L.-X. Zhao, P. Deng, X. Gong, X.-H. Kang and J.-H. Cheng, *ACS Catal.*, 2022, **12**, 7877.

5 For selected examples, see: (*a*) J. Oyamada, M. Nishiura and Z. Hou, *Angew. Chem., Int. Ed.*, 2011, **50**, 10720; (*b*) P. Ricci, K. Krämer and L. Larrosa, *J. Am. Chem. Soc.*, 2014, **136**, 18082; (*c*) D. A. Frasco, S. Mukherjee, R. D. Sommer, C. M. Perry, N. S. Lambic, K. A. Abboud, E. Jakubikova and E. A. Ison, *Organometallics*, 2016, **35**, 2435; (*d*) C. Xue, Y. Luo, H.-L. Teng, Y.-H. Ma, M. Nishiura and Z. Hou, *ACS Catal.*, 2018, **8**, 5017; (*e*) W. Xu, X. Cong, K. An, S.-J. Lou, Z. Li, M. Nishiura, T. Murahashi and Z. Hou, *Angew. Chem., Int. Ed.*, 2022, **61**, e202210624.

6 R. Mandal, B. Garai and B. Sundararaju, *ACS Catal.*, 2022, **12**, 3452.

7 For the reviews on the application of rare-earth organic complexes in organic synthesis, see: (*a*) X. Zhang and J. Jiang, in *Rare Earth Coordination Chemistry*, ed. C. Huang, Wiley-VCH, Weinheim, 2010, ch. 4, p. 138; (*b*) M. Zimmermann and R. Anwander, *Chem. Rev.*, 2010, **110**, 6194; (*c*) R. Waterman, *Organometallics*, 2013, **32**, 7249; (*d*) K. R. D. Johnsona and P. G. Hayes, *Chem. Soc. Rev.*, 2013, **42**, 1947; (*e*) M. Nishiura, F. Guo and Z. Hou, *Acc. Chem. Res.*, 2015, **48**, 2209; (*f*) P. Gandeepan, T. Müller, D. Zell, G. Cera, S. Warratz and L. Ackermann, *Chem. Rev.*, 2019, **119**, 2192.

8 For the reviews on C–H functionalization promoted by rare-earth alkyl complexes, see: (*a*) H. Tsurugi, K. Yamamoto, H. Nagae, H. Kanekoa and K. Mashima, *Dalton Trans.*, 2014, **43**, 2331; (*b*) J. Hannedouche and E. Schulz, *Organometallics*, 2018, **37**, 4313; (*c*) Q. Sun, X. Xu and X. Xu, *ChemCatChem*, 2022, e202201083; (*d*) M. Inoue, H. Tsurugi and K. Mashima, *Coord. Chem. Rev.*, 2022, **473**, 214810; (*e*) K. Seth, *Org. Chem. Front.*, 2022, **9**, 3102.

9 For selected examples of polymerization reactions promoted by rare-earth alkyl complexes, see: (*a*) Y. Matsuo, K. Mashima and K. Tani, *Organometallics*, 2001, **20**, 3510; (*b*) Z. Hou, in *Multimetallic Catalysts in Organic Synthesis*, eds M. Shibasaki and Y. Yamamoto, WILEY-VCH, Weinheim, 2004, ch. 6, p. 143; (*c*) K. Beckerle and J. Okuda, in *Syndiotactic Polystyrene*, ed. J. Schellenberg, WILEY-VCH, Weinheim, 2009, ch. 7, p. 125; (*d*) Z.-B. Jian and D.-M. Cui, *Dalton Trans.*, 2012, **41**, 2367; (*e*) P. Xu, Y. Yao and X. Xu, *Chem. – Eur. J.*, 2017, **23**, 1263; (*f*) Y. Yang, H. Wang, L. Huang, M. Nishiura, Y. Higaki and Z. Hou, *Angew. Chem., Int. Ed.*, 2021, **60**, 26192.

10 (*a*) Y. Chen, D. Song, J. Li, X. Hu, X. Bi, T. Jiang and Z. Hou, *ChemCatChem*, 2018, **10**, 159; (*b*) A. Kundu, M. Inoue, H. Nagae, H. Tsurugi and K. Mashima, *J. Am. Chem. Soc.*, 2018, **140**, 7332; (*c*) B. Tang, X.-Y. Hu, C.-L. Liu, T. Jiang, F. Alam and Y.-H. Chen, *ACS Catal.*, 2019, **9**, 599; (*d*) J. Su, Y. Zhou and X. Xu, *Org. Biomol. Chem.*, 2019, **17**, 2013; (*e*) J.-H. Su, Y.-C. Luo and X. Xu, *Chem. Commun.*, 2021, **57**, 3688.

11 For the reviews on *N*-heterocyclic iminato ligands, see: (*a*) A. Trambitas, T. Panda and M. Tamm, *Z. Anorg. Allg. Chem.*, 2010, **636**, 2156; (*b*) X. Wu and M. Tamm, *Coord. Chem. Rev.*, 2014, **260**, 116; (*c*) T. Ochiai, D. Franz and S. Inoue, *Chem. Soc. Rev.*, 2016, **45**, 6327; (*d*) A. Doddi, M. Peters and M. Tamm, *Chem. Rev.*, 2019, **119**, 6994; (*e*) S. Revathi, P. Raja, S. Saha, M. S. Eisen and T. Ghatak, *Chem. Commun.*, 2021, **57**, 5483.

12 T. K. Panda, S. Randoll, C. G. Hrib, P. G. Jones, T. Bannenberg and M. Tamm, *Chem. Commun.*, 2007, 5007.

13 A. G. Trambitas, T. K. Panda, J. Jenter, P. W. Roesky, C. Daniliuc, C. G. Hrib, P. G. Jones and M. Tamm, *Inorg. Chem.*, 2010, **49**, 2435.

14 (*a*) B. D. Stubbert and T. J. Marks, *J. Am. Chem. Soc.*, 2007, **129**, 4253; (*b*) S. D. Wobser and T. J. Marks, *Organometallics*, 2013, **32**, 2517; (*c*) S. Saha and M. S. Eisen, *ACS Catal.*, 2019, **9**, 5947.

15 (*a*) E. Barnea, D. Moradove, J. C. Berthet, M. Ephritikhine and M. S. Eisen, *Organometallics*, 2006, **25**, 320; (*b*) W.-P. Zhao, B.-B. Wang, B. Dong, H. Liu, Y.-M. Hu, M. S. Eisen and X.-Q. Zhang, *Organometallics*, 2020, **39**, 3983.

16 Imidazolin-2-imines are guanidine derivatives, which have been employed as an important type of ligands and catalysts in organometallic chemistry of rare-earth elements and organic synthesis. For selected reviews, see: (*a*) F. T. Edelmann, *Chem. Soc. Rev.*, 2012, **41**, 7657; (*b*) S. X. Dong, X. M. Feng and X. H. Liu, *Chem. Soc. Rev.*, 2018, **47**, 8525; (*c*) H.-C. Chou, D. Leow and C.-H. Tan, *Chem.–Asian J.*, 2019, **14**, 3803.

17 For a detailed comparison with related rare–earth alkyl complexes supported by imidazolin-2-iminato ligands, see ESI,† Page 34 for more details.

18 The calculated Wiberg bond order of Sc–Nimido is 1.32 in Chen's work, see: (*a*) E. Lu, Y.-X. Li and Y.-F. Chen, *Chem. Commun.*, 2010, **46**, 4469; (*b*) E. Lu, J.-X. Chu and Y.-F. Chen, *Acc. Chem. Res.*, 2018, **51**, 557.

19 In the following investigation, **Sc-1** was superior than **Sc-2** and **Sc-6** in the reactions of 2-methyl anisoles with styrenes. therefore, **Sc-1** was selected as the optimal catalyst for the examination of substrate scope.

20 S. Gatard, R. Çelenligil-Çetin, C.-Y. Guo, B. M. Foxman and O. V. Ozerov, *J. Am. Chem. Soc.*, 2006, **128**, 2808.

21 F. Liu, G. Luo, Z. Hou and Y. Luo, *Organometallics*, 2017, **36**, 1557.

22 Y. Luo, Y.-H. Ma and Z. Hou, *J. Am. Chem. Soc.*, 2018, **140**, 114.

23 For more details, see ESI,† Page 15–18.

24 Y. Zhou, P. Wu, F.-S. Cao, L. Shi, N. Zhang, Z.-G. Xue and G. Luo, *RSC Adv.*, 2022, **12**, 13593.

25 S. J. Wang, C. F. Zhang, D. Li, Y. Q. Zhou, Z. S. Su, X. M. Feng and S. X. Dong, *Sci. China: Chem.*, 2023, **66**, 147.